

## Tunable Quantum Criticality in Multicomponent Rydberg Arrays

Chepiga, Natalia

**DOI**

[10.1103/PhysRevLett.132.076505](https://doi.org/10.1103/PhysRevLett.132.076505)

**Publication date**

2024

**Document Version**

Final published version

**Published in**

Physical review letters

**Citation (APA)**

Chepiga, N. (2024). Tunable Quantum Criticality in Multicomponent Rydberg Arrays. *Physical review letters*, 132(7), Article 076505. <https://doi.org/10.1103/PhysRevLett.132.076505>

**Important note**

To cite this publication, please use the final published version (if applicable). Please check the document version above.

**Copyright**

Other than for strictly personal use, it is not permitted to download, forward or distribute the text or part of it, without the consent of the author(s) and/or copyright holder(s), unless the work is under an open content license such as Creative Commons.

**Takedown policy**

Please contact us and provide details if you believe this document breaches copyrights. We will remove access to the work immediately and investigate your claim.

## Tunable Quantum Criticality in Multicomponent Rydberg Arrays

Natalia Chepiga 

*Kavli Institute of Nanoscience, Delft University of Technology, Lorentzweg 1, 2628 CJ Delft, The Netherlands*



(Received 18 September 2023; revised 27 November 2023; accepted 23 January 2024; published 15 February 2024)

Arrays of Rydberg atoms have appeared as a remarkably rich playground to study quantum phase transitions in one dimension. One of the biggest puzzles that was brought forward in this context are chiral phase transitions out of density waves. Theoretically predicted chiral transition out of period-four phase is still pending experimental verification mainly due to extremely short interval over which this transition is realized in a single-component Rydberg array. In this Letter, we show that multicomponent Rydberg arrays with extra experimentally tunable parameters provide a mechanism to manipulate quantum critical properties without breaking translation symmetry explicitly. We consider an effective blockade model of two component Rydberg atoms. Weak and strong components obey nearest- and next-nearest-neighbor blockades correspondingly. When laser detuning is applied to either of the two components the system is in the period-3 and period-2 phases. But laser detuning applied to both components simultaneously stabilizes the period-4 phase partly bounded by the chiral transition. We show that relative ratio of the Rabi frequencies of the two components tunes the properties of the conformal Ashkin-Teller point and allows us to manipulate an extent of the chiral transition. The prospects of multicomponent Rydberg arrays in the context of critical fusion is briefly discussed.

DOI: [10.1103/PhysRevLett.132.076505](https://doi.org/10.1103/PhysRevLett.132.076505)

*Introduction.*—Understanding the nature of quantum phase transitions in low-dimensional systems is a central topic of condensed matter physics [1,2]. One of the most debated and long-standing problems in the theory of phase transitions is a chiral melting of the density-wave order that roots back to the study of adsorbed monolayers [3–9]. Recent experiments on Rydberg atoms attract new attention to this problem now in the context of one-dimensional (1D) quantum chains [10–18]. The microscopic Hamiltonian of a Rydberg array can be formulated in terms of hard-core bosons:

$$H_{\text{Ryd}} = \sum_i \left[ -\Omega(d_i^\dagger + d_i) - \Delta n_i + \sum_{R=1}^{+\infty} V_R n_i n_{i+R} \right], \quad (1)$$

where  $\Omega$  is a Rabi frequency and  $V_R \propto R^{-6}$  is the van der Waals potential. The competition between the laser detuning  $\Delta$  that keeps atom in a Rydberg state and strong van der Waals interaction that blocks simultaneous excitation of multiple atoms within a certain radius realizes a sequence of density-wave lobes with integer periodicities  $p = 2, 3, 4, \dots$  [10,18]. These ordered phases are surrounded by the disordered phase with incommensurate short-range order. Incommensurability signals chiral perturbations in a system that have a drastic effect on the nature of quantum phase transitions [7,9,19].

For  $p = 2$  chiral perturbations do not appear and the transition, if continuous, is in the Ising universality class. For  $p \geq 5$  the transition takes place via an incommensurate

Luttinger liquid phase (also known as a floating phase) [18]. The transition out of the  $p = 3$  phase is more complicated. Inside the disordered phase chiral perturbations vanish along commensurate lines with wave vectors  $q = 2\pi/p$ . At the point where a commensurate line hits the boundary of the period-3 phase the transition is conformal in the three-state Potts universality class. Away from this point chiral perturbations are relevant and the transition is believed to be in the Huse-Fisher chiral universality class [9,12–14,17]. When chiral perturbations are strong a chiral transition is eventually replaced by a floating phase [12,13,18].

The most intriguing case is  $p = 4$ . Along the commensurate line  $q = \pi/2$  the transition is conformal [15], however, the underlying Ashkin-Teller critical theory forms a *weak* universality class [20,21]. This implies that critical exponents, for instance  $\nu$  that describes a divergence of the correlation length, can be continuously tuned by an external parameter  $\lambda$  [20]. The Ashkin-Teller model interpolates between two decoupled Ising chains at  $\lambda = 0$  and the symmetric four-state Potts point at  $\lambda = 1$  (see Fig. 1). The exponent  $\nu$  as a function of  $\lambda$  is known exactly [20,22]:

$$\nu = \frac{1}{2 - \frac{\pi}{2} [\arccos(-\lambda)]^{-1}}.$$

As sketched in Fig. 1 the effect of chiral perturbations that appear in Rydberg arrays away from the commensurate line change the nature of the transition [3,9,23,24]. When  $\nu \gtrsim 0.8$  chiral perturbations immediately open a floating

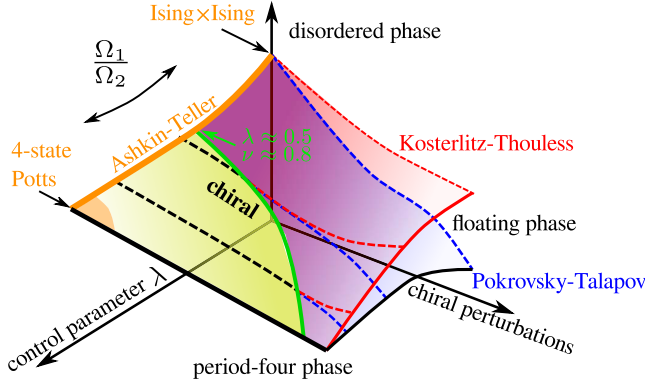


FIG. 1. Nature of the quantum phase transition between the period-four and disordered phases. Vertical axis states for some relevant operator that brings a system from the disordered phase to the period-4 phase. Orange line states for the conformal Ashkin-Teller transition. Yellow and orange regions at finite chiral perturbations correspond to direct chiral and Ashkin-Teller transitions. Blue and red surfaces indicate Pokrovsky-Talapov and Kosterlitz-Thouless transitions with a floating phase between the two. Green line states for the Lifshitz line.

phase; when  $0.8 \gtrsim \nu \geq (1 + \sqrt{3})/4$  chiral perturbations are also relevant but for a while the transition is direct in the chiral universality class [23,24]; finally, when  $(1 + \sqrt{3})/4 > \nu \geq 2/3$  chiral perturbations are irrelevant and for a certain interval the transition is in the Ashkin-Teller universality class that upon increasing chiral perturbations is followed first by the chiral transition and then by the floating phase [24,25]. In the single-component Rydberg array the conformal Ashkin-Teller point has critical exponent  $\nu \approx 0.78$  and the second scenario is realized [15]. However, as illustrated in Fig. 1, the closer is the Ashkin-Teller point to  $\nu \approx 0.8$  the shorter is the interval of the chiral transition. As a consequence, the chiral transition in a Rydberg array appears only very close to the conformal point [13] making its experimental investigation extremely difficult.

In this Letter we directly address this problem and show how to manipulate quantum critical properties and to enlarge an extent of the chiral transition with two-component bosonic Rydberg array (see below). We show that the ratio between Rabi frequencies of the two components tunes the properties of the Ashkin-Teller multicritical point that in turn controls an appearance and an extent of the chiral transition.

**Multicomponent Rydberg atoms.**—Rydberg arrays defined in Eq. (1) have two independent parameters while the phase diagram of the chiral Ashkin-Teller model [24] sketched in Fig. 1 requires at least three. In recent years there were several proposals aiming to extend the set of control parameters in Rydberg atoms [26–32]. Among them the multispecies [26,27] and the multicomponent [28,29] Rydberg arrays seem the most promising. In multispecies setup a certain arrangement of Cs and Rb atoms is prepared. Rabi frequency, laser detuning, and van der Waals potential can be individually controlled for each

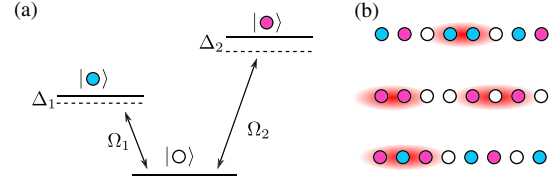


FIG. 2. Sketch of the two-component Rydberg atom. (a) Atoms are excited to the two Rydberg levels  $\alpha = 1, 2$  from the ground state by a laser with Rabi frequency  $\Omega_\alpha$  and detuning  $\Delta_\alpha$ . (b) Interaction within the strong (magenta) and weak (blue) components result in nearest- and next-nearest-neighbor blockades. Configurations that violate these blockades are marked with red ellipses.

individual specimen in addition to the interspecies interaction, so the effective model spans over six-dimensional parameter space. In multicomponent Rydberg atoms, only one type of atom is used but each atom can be excited to one of the two Rydberg levels components as sketched in Fig. 2. The levels can be selected such that (i) first-component interaction is much stronger than the second component one; and (ii) all other interactions including those between different components are negligibly small. This model has five independent parameters: interatomic spacing, two Rabi frequencies  $\Omega_1$  and  $\Omega_2$  and two individually controlled laser detunings  $\Delta_1$  and  $\Delta_2$  (see Fig. 2). Between two setups—multispecies and multicomponent arrays—the latter has one significant advantage in the context of quantum phase transition and chiral melting: it preserves translation symmetry.

**The blockade model.**—Because of the very fast increase of the van der Waals potential at short distances simultaneous occupation of atoms within certain blockade radius is essentially excluded. It allows us to approximate long-range interactions of two components with two types of Rydberg blockade: nearest-neighbor blockade for the weak and next-nearest-neighbor one for the strong components. This effectively fixes two parameters—relative interaction strength of two species and an interatomic distance. The resulting model is defined by the following microscopic Hamiltonian acting in a constrained Hilbert space:

$$H_{MC} = \sum_{\alpha=1,2} \sum_i [-\Omega_\alpha (d_{\alpha,i}^\dagger + d_{\alpha,i}) - \Delta_\alpha n_{\alpha,i}], \quad (2a)$$

$$n_{1,i} n_{1,i+1} = n_{2,i} n_{2,i+1} = n_{2,i} n_{2,i+2} = n_{1,i} n_{2,i} = 0. \quad (2b)$$

Here,  $d_{\alpha,i}^\dagger$  brings an atom at site  $i$  from the ground state to a first or second Rydberg level if  $\alpha = 1$  or  $2$  correspondingly. This model has three independent parameters that we define as  $\Delta_1/\Omega_1$ ,  $\Delta_2/\Omega_2$ , and  $\Omega_1/\Omega_2$ . We study the model with a state-of-the-art density-matrix renormalization group algorithm [33–36] with up to  $N = 907$  sites keeping up to 2500 states and performing up to 8 sweeps (see Supplemental Material [37] for details).

**Phase diagram.**—Our main results are summarized in three phase diagrams in Fig. 3. When laser detunings are small  $\Delta_1/\Omega_1, \Delta_2/\Omega_2 \ll 1$  the system is in the disordered phase and translation symmetry is not broken. For  $\Delta_2/\Omega_2 \gg \Delta_1/\Omega_1$  the system is populated with the strong component that due to next-nearest-neighbor Rydberg blockade leads to a period-three phase separated from the disorder phase by either chiral transition or the floating phase [37]. In the opposite limit  $\Delta_2/\Omega_2 \ll \Delta_1/\Omega_1$  the system is in the period-two phase with every other site occupied by a weak component; the transition to the disordered phase is in the Ising universality phase [37]. Upon increasing the detuning  $\Delta_2$  the system undergoes the second Ising transition [37] where the translation symmetry is spontaneously broken once again and every other empty site of the period-2 phase is occupied by the strong component resulting in the period-four phase [sketched in Fig. 3(a)] with broken  $\mathbb{Z}_2 \times \mathbb{Z}_2$  symmetry (see Supplemental Material [37] for further details). Upon increasing  $\Delta_2/\Omega_2$  two Ising lines come closer and eventually merge into a multicritical point in the Ashkin-Teller universality class [21]. Beyond this point the transition from the disordered to the period-four phases is either direct in the chiral universality class or via the floating phase as shown in Fig. 3. This is further supported by incommensurate correlations that weak component develops beyond the disorder line [37].

We distinguish three types of transitions—Ashkin-Teller, chiral, and floating phase—by looking at the product  $|q - \pi/2| \times \xi$ , where  $q$  is incommensurate wave vector approaching its commensurate value with the critical exponent  $\beta$  and  $\xi$  is a correlation length diverging with the critical exponent  $\nu$ . To the best of our knowledge for the Ashkin-Teller criticality the exact value of  $\bar{\beta}$  is not known but according to Huse and Fisher  $\bar{\beta} > \nu$  [7,9]. Then for the Ashkin-Teller point the product  $|q - \pi/2| \times \xi$  is expected to vanish. By contrast, at the chiral transition the equality  $\nu = \bar{\beta}$  should hold and  $|q - \pi/2| \times \xi$  takes some finite value. In the case of the floating phase, it is separated from the disordered phase by the Kosterlitz-Thouless transition [40] characterized by the stretch-exponential divergence of correlation length; at the same time the wave vector  $q$  remains incommensurate across the transition, therefore  $|q - \pi/2| \times \xi$  diverges.

In Fig. 4 we show the inverse of the correlation length and the product  $|q - \pi/2| \times \xi$  across different cuts through the transition. For  $\Omega_1/\Omega_2 = 1$  and  $\Delta_2/\Omega_2 = 2.27$  presented in Figs. 4(a) and 4(b) the divergence of the correlation length is symmetric and the numerically extracted critical exponent  $\nu = \nu' \approx 0.76 \pm 0.02$  is consistent with the Ashkin-Teller critical theory; the product  $|q - \pi/2| \times \xi$  vanishes. This Ashkin-Teller point belongs to the interval where chiral perturbations result into a chiral transition [23,24]. Indeed, already at  $\Delta_2/\Omega_2 = 2.3$  the product  $|q - \pi/2| \times \xi$  shown in Fig. 4(c) takes some finite value at the transition. This picture remains valid up to  $\Delta_2/\Omega_2 = 2.5$ . The location of the

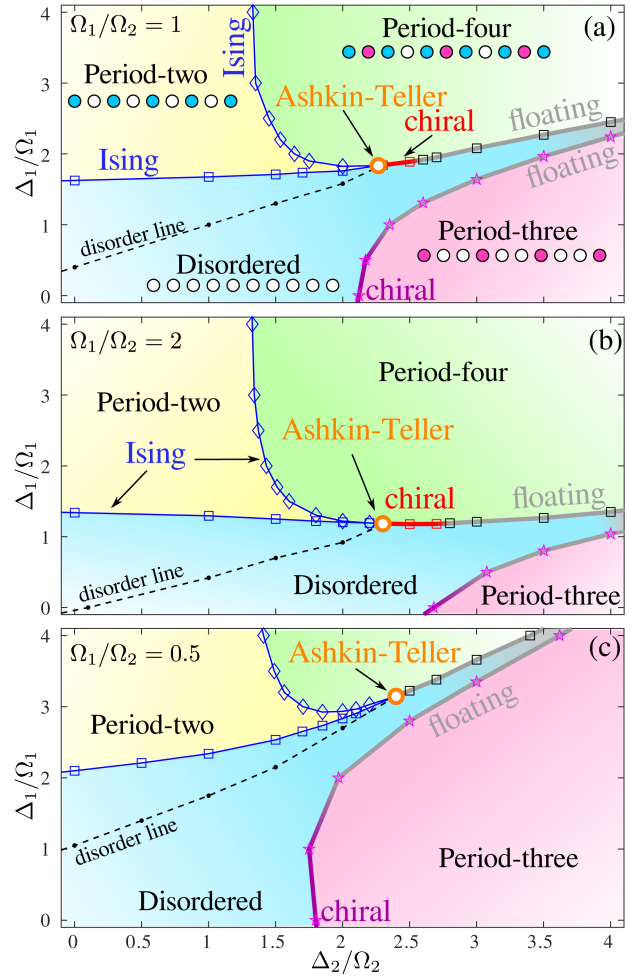


FIG. 3. Phase diagrams of the blockade models defined by Eqs. (2a) and (2b) as a function of laser detuning of two species and for three relative ratio of Rabi frequencies  $\Omega_1/\Omega_2$ . Each phase diagram contains four gapped phases: the disordered phase, and three density wave phases with periodicity  $p = 2, 3$ , and 4. Typical patterns of these phases are sketched in (a) where white circles denote atoms in the ground state, and blue and red circles denote the states for atoms excited to the first (weak) and second (strong) Rydberg levels, correspondingly. The period-2 phase is separated from the disordered and period-4 phases by two Ising transitions (blue squares and diamonds). The multicritical point (open orange circle) belongs to the Ashkin-Teller universality class. For some interval in (a) and (b) the transition to the period-4 phase is direct and chiral (red line). The key observation is that the extent of the chiral transition in (b) for  $\Omega_1/\Omega_2 = 2$  is significantly larger than in (a) for  $\Omega_1/\Omega_2 = 1$ , while for  $\Omega_1/\Omega_2 = 0.5$  in (c) the floating phase (gray) opens immediately. The transition between the period-three phase and the disordered phase is chiral (purple line) for small values of  $\Delta_1/\Omega_1$  and through a floating phase (gray) for large detuning of the weak component (see “Methods” for details).

transition is extracted by fitting the correlation length in the period-four phase [37]. For  $\Delta_2/\Omega_2 = 2.6$  presented in Fig. 4(d) we see a sign of divergence of  $|q - \pi/2| \times \xi$  signaling the opening of the floating phase.

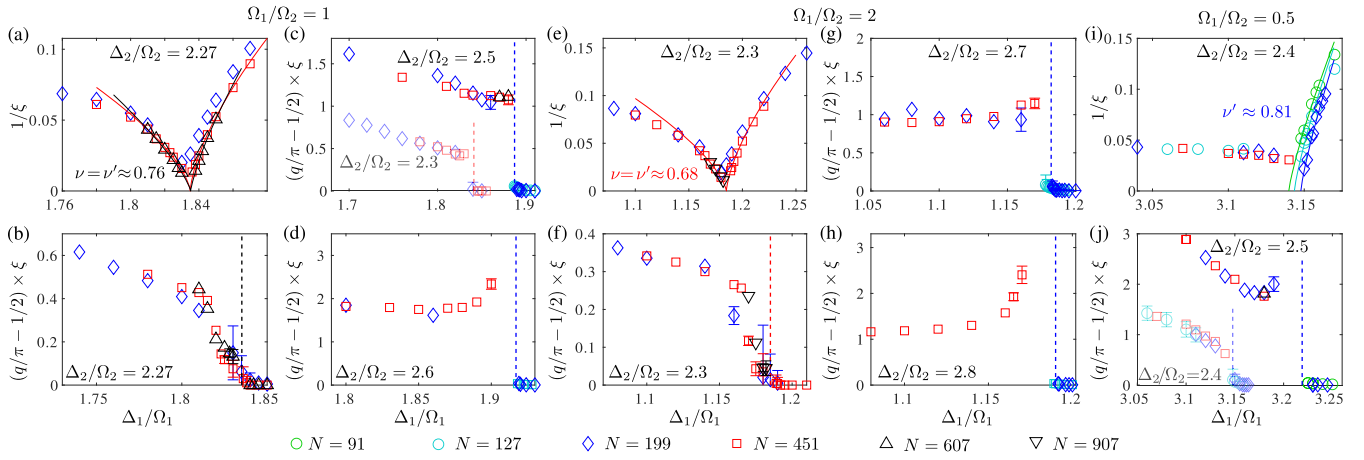


FIG. 4. Inverse correlation length  $1/\xi$  and product  $|q - \pi/2| \times \xi$  along various cuts across the transition (a)–(d) for  $\Omega_1/\Omega_2 = 1$ ; (e)–(h) for  $\Omega_1/\Omega_2 = 2$ ; and (i), (j) for  $\Omega_1/\Omega_2 = 0.5$ . (a), (b), (e), (f), (i) and pale symbols in (j): vertical cut through the Ashkin-Teller point. (c), (g): vertical cuts through chiral transitions. (d), (h) and bright symbols in (j): a cut through a floating phase. In (a) and (e) correlation lengths are fitted with the power law with equal critical exponents  $\nu = \nu'$  specified in each panel.  $|q - \pi/2| \times \xi$  is defined with error bars  $2 \times \xi^2/N^2$ ; we only show error bars if they exceed the size of the symbols. Dashed lines show the boundary of the ordered phase extracted by fitting the correlation length, color code corresponds to the legend in the lower part of the figure.

For the larger ratio of Rabi frequencies  $\Omega_1/\Omega_2 = 2$  the location of the Ashkin-Teller point is almost the same but the extracted critical exponent is noticeably smaller  $\nu \approx 0.68 \pm 0.04$  [see Figs. 4(e) and 4(f)]. Beyond this point we detect the chiral transition that extends at least up to  $\Delta_2/\Omega_2 = 2.7$  as shown in Fig. 4(g). In Fig. 4(h) for  $\Delta_2/\Omega_2 = 2.8$  one can clearly see a divergence of  $|q - \pi/2| \times \xi$  upon approaching the floating phase. The larger interval of the chiral transition compares to the previous case with  $\Omega_1/\Omega_2 = 1$  being fully consistent with the smaller critical exponent  $\nu$  at the Ashkin-Teller point [see Fig. 4(e)]. In other words, by increasing  $\Omega_1/\Omega_2$  one can tune the multicritical Ashkin-Teller point toward larger  $\lambda$  and smaller  $\nu$ , that in turn leads to a longer chiral transition as sketched in Fig. 1. Note also that the difference between the chiral transition and floating phase is more pronounced for  $\Omega_1/\Omega_2 = 2$ .

For  $\Omega_1/\Omega_2 = 0.5$  the multicritical point is very close to the period-three phase and the floating phase surrounding it; as a consequence the correlation length is very large all over the narrow window of the disordered phase. This prevents us from fitting the divergence of the correlation length inside the disordered phase but the product  $|q - \pi/2| \times \xi$  computed locally remains a valid measure: it goes to zero at the Ashkin-Teller point at  $\Delta_2/\Omega_2 = 2.4$  [see Figs. 4(i)–4(j)], while for  $\Delta_2/\Omega_2 = 2.5$  it already shows a signature of divergence suggesting the presence of the floating phase. The latter is further supported by the divergence of the correlation length with the Pokrovsky-Talapov critical exponent  $1/2$  (see Supplemental Material [37]). The picture is completed by the observation that along the cut  $\Delta_2/\Omega_2 = 2.4$  through the Ashkin-Teller point the correlation length diverges with the critical exponent  $\nu' \approx 0.81$  that lies outside of the interval  $2/3 \leq \nu \lesssim 0.8$

where chiral transition is possible. Of course, neither this interval nor the critical exponents  $\nu'$  are exact and we cannot exclude a possibility of a short chiral transition between  $\Delta_2/\Omega_2 = 2.4$  and  $2.5$ . But what we observe here is a very important tendency of the Ashkin-Teller critical exponent to increase with decreasing  $\Omega_1/\Omega_2$  such that the chiral transition shrinks to the point when it eventually disappears.

*Discussion.*—To summarize, our results offer a novel approach to manipulate quantum criticality in Rydberg atoms that, in particular, overcomes the bottleneck associated with the short extent of the chiral transition. In addition, we formulate a protocol to probe the complete phase diagram of the chiral Ashkin-Teller model. Altogether, these provide an opportunity to explore universal and nonuniversal properties of chiral transitions—a necessary step toward a formal definition of the  $p = 4$  chiral universality class. We expect our results obtained for the blockade approximation to be qualitatively correct for the model with  $1/r^6$  potential as soon as the selected Rydberg levels and the lattice spacing are such that detuning of weak and strong components alone leads to stable period-two and period-three phases correspondingly. Multicomponent Rydberg arrays open a unique opportunity to explore fusion rules of quantum criticalities directly on a lattice. Here, we focused on the simplest case: fusion of two Ising transitions into the Ashkin-Teller point followed by the chiral transition. Playing with different interaction regimes and longer blockades one can realize, for instance, a fusion of chiral transitions. Further generalization to three and more components is conceptually straightforward and introduces a new class of models with multicomponent Hilbert space. Multiple individually controllable parameters enables a fine-tuning, for instance, to points with higher symmetries.

I thank Bernhard Lüscher, Samuel Nyckees, and Frederic Mila for insightful discussions on the chiral Ashkin-Teller model and Jiri Minar for inspiring discussion on multicomponent Rydberg arrays. This work has been supported by the Delft Technology Fellowship and it was performed in part at Aspen Center for Physics, which is supported by National Science Foundation Grant No. PHY-2210452. Numerical simulations have been performed at the DelftBlue HPC and at the Dutch national e-infrastructure with the support of the SURF Cooperative.

- 
- [1] T. Giamarchi, *Quantum Physics in One Dimension*, International Series of Monographs on Physics (Clarendon Press, Oxford, 2004).
- [2] A. M. Tsvelik, *Quantum Field Theory in Condensed Matter Physics*, 2nd ed. (Cambridge University Press, Cambridge, 2003).
- [3] M. den Nijs, *Phase Transitions Crit. Phenom.* **12**, 219 (1988).
- [4] J. Schreiner, K. Jacobi, and W. Selke, *Phys. Rev. B* **49**, 2706 (1994).
- [5] D. L. Abernathy, S. Song, K. I. Blum, R. J. Birgeneau, and S. G. J. Mochrie, *Phys. Rev. B* **49**, 2691 (1994).
- [6] W. Selke and J. M. Yeomans, *Z. Phys. B* **46**, 311 (1982).
- [7] D. A. Huse and M. E. Fisher, *Phys. Rev. Lett.* **49**, 793 (1982).
- [8] D. A. Huse, A. M. Szpilka, and M. E. Fisher, *Physica (Amsterdam)* **121A**, 363 (1983).
- [9] D. A. Huse and M. E. Fisher, *Phys. Rev. B* **29**, 239 (1984).
- [10] A. Keesling, A. Omran, H. Levine, H. Bernien, H. Pichler, S. Choi, R. Samajdar, S. Schwartz, P. Silvi, S. Sachdev, P. Zoller, M. Endres, M. Greiner, V. Vuletić, and M. D. Lukin, *Nature (London)* **568**, 207 (2019).
- [11] N. Chepiga and F. Mila, *SciPost Phys.* **6**, 33 (2019).
- [12] N. Chepiga and F. Mila, *Phys. Rev. Lett.* **122**, 017205 (2019).
- [13] I. A. Maceira, N. Chepiga, and F. Mila, *Phys. Rev. Res.* **4**, 043102 (2022).
- [14] G. Giudici, A. Angelone, G. Magnifico, Z. Zeng, G. Giudice, T. Mendes-Santos, and M. Dalmonte, *Phys. Rev. B* **99**, 094434 (2019).
- [15] N. Chepiga and F. Mila, *Nat. Commun.* **12**, 414 (2021).
- [16] S. Whitsitt, R. Samajdar, and S. Sachdev, *Phys. Rev. B* **98**, 205118 (2018).
- [17] R. Samajdar, S. Choi, H. Pichler, M. D. Lukin, and S. Sachdev, *Phys. Rev. A* **98**, 023614 (2018).
- [18] M. Rader and A. M. Läuchli, *arXiv:1908.02068*.
- [19] S. Ostlund, *Phys. Rev. B* **24**, 398 (1981).
- [20] M. Kohmoto, M. den Nijs, and L. P. Kadanoff, *Phys. Rev. B* **24**, 5229 (1981).
- [21] P. Di Francesco, P. Mathieu, and D. Sénéchal, *Conformal Field Theory*, Graduate Texts in Contemporary Physics (Springer, New York, 1997).
- [22] A. O'Brien, S. D. Bartlett, A. C. Doherty, and S. T. Flammia, *Phys. Rev. E* **92**, 042163 (2015).
- [23] S. Nyckees and F. Mila, *Phys. Rev. Res.* **4**, 013093 (2022).
- [24] B. Lüscher, F. Mila, and N. Chepiga, *Phys. Rev. B* **108**, 184425 (2023).
- [25] H. J. Schulz, *Phys. Rev. B* **28**, 2746 (1983).
- [26] K. Singh, S. Anand, A. Pocklington, J. T. Kemp, and H. Bernien, *Phys. Rev. X* **12**, 011040 (2022).
- [27] C. Sheng, J. Hou, X. He, K. Wang, R. Guo, J. Zhuang, B. Mamat, P. Xu, M. Liu, J. Wang, and M. Zhan, *Phys. Rev. Lett.* **128**, 083202 (2022).
- [28] E. Levi, J. Minář, J. P. Garrahan, and I. Lesanovsky, *New J. Phys.* **17**, 123017 (2015).
- [29] Z. Lan, W. Li, and I. Lesanovsky, *Phys. Rev. A* **94**, 051603(R) (2016).
- [30] L. Eck and P. Fendley, *Phys. Rev. B* **108**, 125135 (2023).
- [31] B. Beradze, M. Tsitsishvili, E. Tirrito, M. Dalmonte, T. Chanda, and A. Nersesyan, *Phys. Rev. B* **108**, 075146 (2023).
- [32] P. Fromholz, M. Tsitsishvili, M. Votto, M. Dalmonte, A. Nersesyan, and T. Chanda, *Phys. Rev. B* **106**, 155411 (2022).
- [33] S. R. White, *Phys. Rev. Lett.* **69**, 2863 (1992).
- [34] U. Schollwöck, *Rev. Mod. Phys.* **77**, 259 (2005).
- [35] S. Ostlund and S. Rommer, *Phys. Rev. Lett.* **75**, 3537 (1995).
- [36] U. Schollwöck, *Ann. Phys. (Amsterdam)* **326**, 96 (2011).
- [37] See Supplemental Material at <http://link.aps.org/supplemental/10.1103/PhysRevLett.132.076505>, which includes Refs. [11,13,15,21,33–36,38,39], for details about the algorithm, further details on various phases, additional numerical results supporting Ising transitions, the extraction of the correlation length and the wave vector, the transition out of period-three phase, the location of the disorder line, and additional results for the transition out of period-four phase.
- [38] L. Ornstein and F. Zernike, *Proc. K. Ned. Akad. Wet. Ser. B* **17**, 793 (1914).
- [39] P. Calabrese and J. Cardy, *J. Phys. A* **42**, 504005 (2009).
- [40] J. M. Kosterlitz and D. J. Thouless, *J. Phys. C* **6**, 1181 (1973).